NASA/CR—2004-213065 GT–2004–53954

Measurements With a Split-Fiber Probe in Complex Unsteady Flows

Jan Lepicovsky
QSS Group, Inc., Cleveland, Ohio

April 2004

The NASA STI Program Office . . . in Profile

Since its founding, NASA has been dedicated to the advancement of aeronautics and space science. The NASA Scientific and Technical Information (STI) Program Office plays a key part in helping NASA maintain this important role.

The NASA STI Program Office is operated by Langley Research Center, the Lead Center for NASA's scientific and technical information. The NASA STI Program Office provides access to the NASA STI Database, the largest collection of aeronautical and space science STI in the world. The Program Office is also NASA's institutional mechanism for disseminating the results of its research and development activities. These results are published by NASA in the NASA STI Report Series, which includes the following report types:

- TECHNICAL PUBLICATION. Reports of completed research or a major significant phase of research that present the results of NASA programs and include extensive data or theoretical analysis. Includes compilations of significant scientific and technical data and information deemed to be of continuing reference value. NASA's counterpart of peer-reviewed formal professional papers but has less stringent limitations on manuscript length and extent of graphic presentations.

- TECHNICAL MEMORANDUM. Scientific and technical findings that are preliminary or of specialized interest, e.g., quick release reports, working papers, and bibliographies that contain minimal annotation. Does not contain extensive analysis.

- CONTRACTOR REPORT. Scientific and technical findings by NASA-sponsored contractors and grantees.

- CONFERENCE PUBLICATION. Collected papers from scientific and technical conferences, symposia, seminars, or other meetings sponsored or cosponsored by NASA.

- SPECIAL PUBLICATION. Scientific, technical, or historical information from NASA programs, projects, and missions, often concerned with subjects having substantial public interest.

- TECHNICAL TRANSLATION. English-language translations of foreign scientific and technical material pertinent to NASA's mission.

Specialized services that complement the STI Program Office's diverse offerings include creating custom thesauri, building customized databases, organizing and publishing research results . . . even providing videos.

For more information about the NASA STI Program Office, see the following:

- Access the NASA STI Program Home Page at ***http://www.sti.nasa.gov***

- E-mail your question via the Internet to help@sti.nasa.gov

- Fax your question to the NASA Access Help Desk at 301–621–0134

- Telephone the NASA Access Help Desk at 301–621–0390

- Write to:
  NASA Access Help Desk
  NASA Center for AeroSpace Information
  7121 Standard Drive
  Hanover, MD 21076

NASA/CR—2004-213065 GT–2004–53954

Measurements With a Split-Fiber Probe in Complex Unsteady Flows

Jan Lepicovsky
QSS Group, Inc., Cleveland, Ohio

Prepared for the
Turbo Expo 2004
sponsored by the American Society of Mechanical Engineers
Vienna, Austria, June 14–17, 2004

Prepared under Contract NAS3–00145

National Aeronautics and
Space Administration

Glenn Research Center

April 2004

Acknowledgments

The work was sponsored by the NASA Glenn Research Center under the Smart Engine Components Project managed by Mr. R.D. Corrigan as a part of the R&T Base Propulsion and Power Program. The author would like to thank Dr. G.E. Welch, NASA GRC, for his continuous support and encouragement during the course of this project.

This work was sponsored by the Low Emissions Alternative Power Project of the Vehicle Systems Program at the NASA Glenn Research Center.

Available from

NASA Center for Aerospace Information
7121 Standard Drive
Hanover, MD 21076

National Technical Information Service
5285 Port Royal Road
Springfield, VA 22100

Available electronically at http://gltrs.grc.nasa.gov

Measurements With a Split-Fiber Probe in Complex Unsteady Flows

Jan Lepicovsky
QSS Group, Inc.
Cleveland, Ohio 44135

ABSTRACT

A split-fiber probe was used to acquire unsteady data in a research compressor. The probe has two thin films deposited on a quartz cylinder *200 μm* in diameter. A split-fiber probe allows simultaneous measurement of velocity magnitude and direction in a plane that is perpendicular to the sensing cylinder. A calibration method was devised for a split-fiber probe, and a new algorithm was developed to decompose split-fiber probe signals into velocity magnitude and direction. The algorithm is based on the minimum value of a merit function that is built over the entire range of flow velocities for which the probe was calibrated. The new decomposition scheme is fast and robust. The split-fiber probe performance and signal decomposition was first verified in a free-jet facility by comparing the data from three thermo-anemometric probes, namely a single-wire, a single-fiber, and the split-fiber probe. The wire and single-fiber probe diameters are *5 μm* and *70 μm*, respectively. All three probes performed extremely well as far as the velocity magnitude was concerned. However, there are differences in the peak values of measured velocity unsteadiness in the jet shear layer. The single-wire probe indicates the highest unsteadiness level, followed closely by the split-fiber probe. The single-fiber probe indicates a noticeably lower level of velocity unsteadiness. Experiments in the NASA Low Speed Axial Compressor facility revealed similar results. The mean velocities agree within *2%* of the measured velocity magnitude. The differences in the measured velocity unsteadiness are similar to the case of a free jet. A reason for these discrepancies is in the different frequency response characteristics of probes used. It follows that the single-fiber probe has the slowest frequency response. In summary, the split-fiber probe worked reliably during the entire program. The acquired data averaged in time followed closely data acquired by conventional pneumatic probes.

Despite small differences among all probes used, that still need to be explained, it is believed that data acquired by the split-fiber probe can be used reliably to analyze unsteady flow phenomena in the NASA Low Speed Axial Compressor.

NOMENCLATURE

Only symbols not sufficiently described in the text are presented here.

d	[*m*]	probe fiber diameter
E	[*V*]	signal voltage
h	[*m*]	blade passage height
R_J	[*m*]	calibration nozzle exit radius
Re	[*1*]	Reynolds number {$Re = (\rho V d)/\mu$}
s_D	[$V.dg^{-1}$]	slope of differential calibration curve
Tu	[*%*]	turbulence intensity
V	[$m.s^{-1}$]	absolute velocity
v'	[$m.s^{-1}$]	velocity fluctuations
W	[$m.s^{-1}$]	relative velocity
y	[*m*]	tangential (pitchwise) direction
z	[*m*]	radial (spanwise) direction
z_D	[*V*]	zero offset of calibration curve
α	[*dg*]	absolute flow angle
β	[*dg*]	relative flow angle
ε	[*dg*]	probe setting angle
η	[*dg*]	probe incidence angle
ρ	[$kg.m^{-3}$]	flow density

Subscripts

A-IN	inlet axial velocity
J	jet
M	magnitude
W	wake

INTRODUCTION

NASA Glenn Research Center conducts a research program to increase the understanding of the complex flow phenomena in axial compressors by obtaining detailed data from a multistage compressor environment for use in developing and verifying models for CFD design codes. The experimental vehicle for this research at the NASA GRC is the Low Speed Axial Compressor (LSAC). The thermo-anemometry technique is employed for unsteady measurements of the axial compressor flowfield.

Thermo-anemometric probes, and in particular hot-wire probes, have been used to measure unsteady velocities for several decades, mainly in one-dimensional low subsonic flows. References to hot-wire anemometry are too numerous to be listed here; an excellent summary of this topic is given in Ref. 1. Use of hot-wire probes in turbomachinery components is much more sporadic (Refs. 2 through 6). The reasons for this are mainly the vulnerability of hot-wire probes in the compressor environment, the restricted temperature range for probe application, and the drop in probe sensitivity to velocity fluctuations with increasing flow temperature and velocity. The operational parameters of the NASA LSAC, especially low flow velocities, and very small total temperature increase, make this facility very suitable for the use of thermo-anemometric probes. At present, all unsteady velocity measurements in the NASA LSAC are made using the thermal anemometry technique, which is the main topic of this paper.

NASA LOW-SPEED MULTISTAGE AXIAL COMPRESSOR

Even though the main focus of this paper is on thermal anemometry, it is believed that the NASA LSAC facility should be introduced first for a better understanding of the approach adopted in selecting the methods of data acquisition. The research compressor consists of a row of inlet guide vanes (IGV) followed by four identical stages, each having a rotor blade row (RBR) and a stator vane row (SVR). The compressor partial cross section, and the blade / vane row layout are shown in Fig. 1. Each rotor has 39 blades, each stator consists of 52 vanes, and there are 52 vanes in the IGV row. The compressor blade tip speed is *61.0 m/s*, and the mean inlet axial flow velocity *24.4 m/s.* (Refs. 7 and 8).

There are two reference frames for a flowfield in turbomachinery components with rotating parts: the relative flow system and the absolute flow system. Variations of flow parameters in the relative flow system, as recorded by an observer sitting on a revolving rotor, differ from flow variations in the absolute flow system, recorded outside of a rotor in a nonmoving frame. The mutual relationship between these two systems is determined by the rotational velocity of the moving rotor. For investigation of rotor flow the relative flow parameters are of interest, because they indicate the performance and efficiency of the component involved. However direct measurements in the relative flow system are extremely difficult and costly. Therefore, the vast majority of turbomachinery measurements is carried out in the absolute flow system, and the results are transformed into the relative flow system computationally.

Flow parameter variations, however, are manifested differently in these two systems; for example variations in velocity magnitude in the relative system are sensed more as variations in velocity direction in the absolute system and vice versa. The situation is illustrated in Fig. 2. The drop in the flow velocity in the blade wake in the relative system (from W to W_W in Fig. 2) is manifested in the absolute system mainly as a change in the velocity vector direction (from V to V_W). Therefore, probes used in the absolute system must have high directional resolution to fully capture the flow unsteadiness.

SCOPE OF INVESTIGATION

The major objective of the work described here was to acquire reliable unsteady velocity data from the NASA LSAC facility. The steady state flow parameters are measured routinely using conventional instrumentation including Kiel probes for total pressures, wedge nulling probes for flow direction and flow static pressures, and static wall taps for

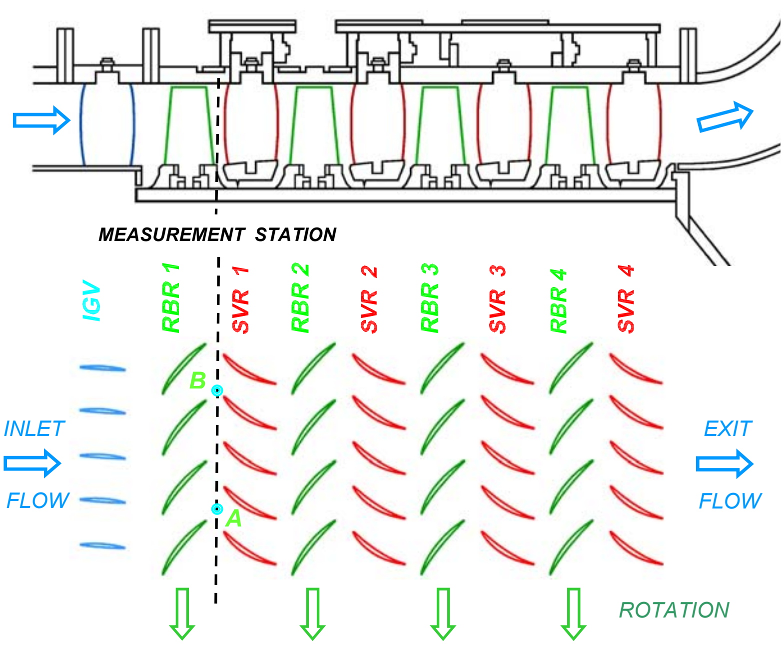

Fig. 1. Flow path and blading plan of the NASA low speed axial compressor.

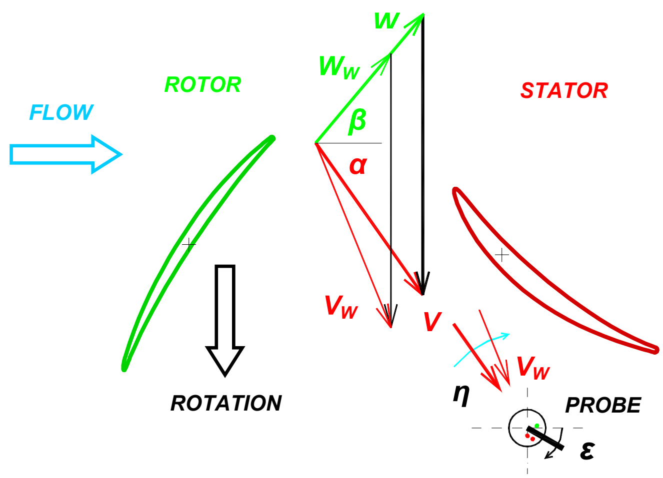

Fig. 2. Velocity triangle and probe setting.

surface static pressures; however, there is a lack of reliable unsteady velocity data acquired in this facility. There were attempts to use thermo-anemometric probes in this facility in the past, but the results achieved were not satisfactory. As explained in the next section, single element (single hot wire) probes do not suffice to acquire data that would describe the rotor flowfield completely. Therefore, two sensor thermo-anemometric probes, as e.g. a split-fiber probe, must be used.

The goal of the first phase was to develop and validate a data reduction technique for split-fiber probes, because we did not have any experience with such probes, and verify reliability of the experimental data acquired. Comparisons with single-fiber and single-wire probe data were made as well as with data from conventional aerodynamic probes. To assess the frequency response of split fiber probes, comparisons with a single-fiber and a single-hot wire probes were made. All the probes used differ in spatial resolution and probe natural frequency. Fig. 3 depicts the characteristic dimensions in the axial-tangential plane of all the probes used, together with the rotor blade trailing edge shape.

In the second phase, we averaged thermo-anemometric probe data and compared data among all thermo-anemometric probes as well as with data taken by conventional aerodynamic probes, for flows in a free-jet facility and in the LSAC facility. In the jet facility, velocity and velocity unsteadiness distributions across a free jet were investigated. In the LSAC facility, radial distributions along the blade span behind the first rotor were examined. We believe that this is an important step to make sure that there is a high degree of correlation among averaged data taken by various probes because it will boost confidence in the accuracy of the unsteady velocity. Nevertheless, we are aware of possible differences due to a lack of specifics about averaging unsteady data by conventional aerodynamic probes, in particular in the LSAC environment.

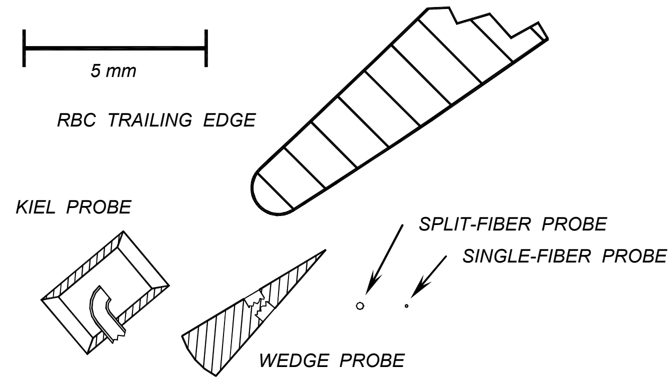

Fig. 3. Comparison of probe sizes.

Finally, in the last phase, the technique of ensemble averaging will be explored and rotor and blade ensemble averages of flow velocity vector in the absolute system will be generated. Also the velocity and angle unsteady data will be converted from the absolute to the relative system. Lastly, the frequency content of unsteady data will be examined using FFT procedures. The last phase is not covered in the present paper, and will be the topic of a follow-up paper.

LIMITATION OF SINGLE-ELEMENT THERMO-ANEMOMETRIC PROBES

The flowfield in axial flow compressors is two-dimensional in the axial-tangential plane over a large midspan portion of the blades. A single-wire probe perpendicular to the axial-tangential plane seems suitable for measuring fluctuations of the velocity magnitude. However, the transformation of velocity fluctuations in the relative system into velocity direction fluctuations in the absolute system imposes a severe limitation on the ability of a single-wire probe to measure the velocity fluctuations. Let us assume a specific case when the conversion from the relative to the absolute system results in velocity V_M that has a constant magnitude and oscillates about a mean direction α by $\pm\Delta\alpha$ (Fig. 4). The velocity components oscillate about V_X by $\pm v_X$ and about V_Y by $\pm v_Y$. Obviously, if the fluctuations v_X and v_Y are measured, the resulting overall fluctuations of the velocity vector V can be calculated and velocity unsteadiness is then a ratio of the overall velocity fluctuations and the velocity magnitude. However, measurement of the velocity vector V_M with a single-wire probe, which is insensitive to flow direction, results in a constant value (the V_M magnitude is constant), and consequently the apparent velocity unsteadiness is zero. This is due to the fact that a single-wire thermo-anemometric probe converts a vector value (magnitude and angle) in to a scalar value (electric voltage proportional to the velocity magnitude). This example clearly illustrates the unconditional necessity to determine both velocity components in the absolute flow system and not only the resulting velocity magnitude.

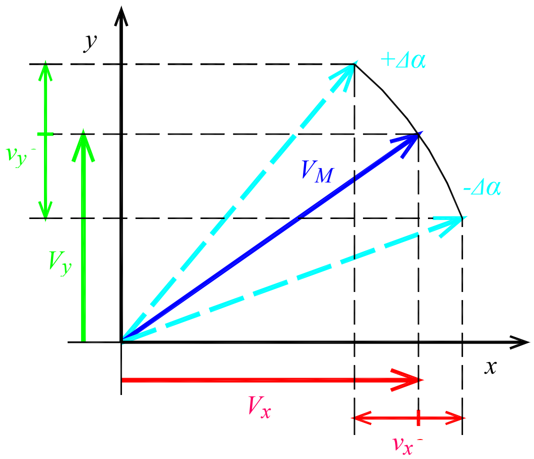

Fig. 4. Oscillation of a velocity vector with constant magnitude.

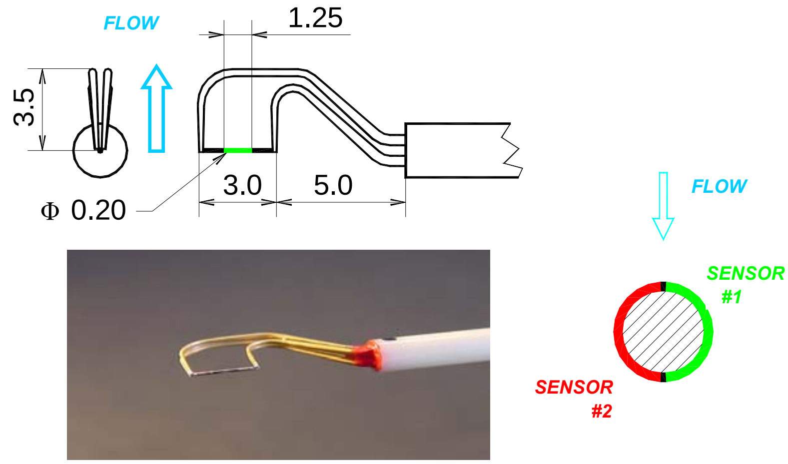

Fig. 5. Split-fiber probe Dantec 55R57 (dimensions in mm).

SPLIT-FIBER THERMO-ANEMOMETRIC PROBES

To measure two velocity components simultaneously requires a two-element probe with two wires oriented at different angles. The main difficulty with this arrangement is the fact that the directional characteristic of an inclined wire is not linear, and is superimposed on a nonlinear velocity characteristic. This complicates the data reduction procedure to decompose the probe signals into velocity components. Further, a two wire probe is even more vulnerable to dust particles in the flow because the probability of a possible wire strike destroying the probe is larger than for a single wire probe.

An alternative approach is to use a split-fiber probe for such measurements. A dual-sensor split-fiber probe resembles a single-wire probe, however instead of a thin wire there is a quartz cylinder placed between the prongs. The diameter of the quartz cylinder (fiber) is *200 µm*. The fiber has two identical nickel-film sensors deposited on its surface. The active length of the sensors is *1.25 mm*. The probe is shown in Fig. 5 (Ref. 9). The cross-section of the fiber indicates the orientation for zero yaw angle. The right sensor facing the flow is labeled #1 (green) and the left one (red) is labeled #2. The probe works like a two-component heated element in connection with a two channel Constant Temperature Anemometer. Because the probe consists of two independent elements, it can be used to measure simultaneously two velocity components (velocity magnitude and velocity angle) in a plane perpendicular to the probe cylinder. Both velocity components are measured simultaneously, which allows determining the Reynolds shear stress component in the unsteady flow. On the other hand, the split-fiber probe diameter is 16 times larger than the diameter of the single-wire probe, which reduces the dynamic response of the split-fiber probe in comparison with a single-wire probe. As discussed later the cut off frequency of the wire probe was determined to be *75 kHz*. A certain reduction in the split-fiber probe frequency response is acceptable, since in the case of the LSAC, the blade passing frequency is only *640 Hz*. The advantage of relatively large hot-element-sensor diameter is that it decreases the probe Knudsen number beyond the threshold above which the molecular effects are important. A practical consequence of this is that the probe can be calibrated in a free-jet flow at ambient conditions, and the velocity data acquired in the compressor do not need to be corrected for slight increases in the air pressure.

VELOCITY CALIBRATION CHARACTERISTICS

Thermo-anemometric probes were calibrated in a free jet flow emanating from a *38-mm* nozzle. The jet stream exits into the atmosphere. The probes were placed *34 mm* downstream of the jet exit plane, and held in an actuator that enabled vertical traversing across the jet stream as well as varying probe yaw angle ±*90 dg* from the axial direction. The velocity calibrations for single-element and dual-element probes are practically identical. A typical velocity calibration curve for a single sensor in terms of throughflow density ρV and the sensor voltage E is shown in Fig. 6. The calibration consists of discrete points that are fitted with a calibration curve. It is this curve that is used for conversion of measured voltages into velocity (or throughflow density) values when the probe is used for testing. Therefore, the probe accuracy depends on the goodness of this fit. Traditionally, this curve fit is based on King's law in the form

$$E^2 = A + B\,(\rho V)^n \qquad \text{(Eq. 1)}$$

where $n = 0.5$ for an infinitely long cylinder in a cross flow. For a short heated wire and additional heat losses through the supporting prongs the value of n is less than 0.5. This law is derived from a heat balance of a probe heated sensor under conditions of forced convection. Seemingly, the constant $A = E_0^2$, has clear physical meaning as the square of the probe voltage at zero flow velocity, which can be easily measured. Once the constant A is known, the constant B and exponent n can be determined from the calibration data by a least squares fit method. The problem is that at zero flow velocity, the heat transfer from the probe sensor is not governed by forced but by free convection. Consequently, the probe voltage at zero flow velocity is higher than it would be for the 'forced' convection at zero flow, and the constant A must be determined by extrapolating forced convection data to zero velocity. In our approach we start with $A = E_0^2$ to determine the first pair of values for B and n. Then we determine the value of a merit function that is equal to the sum of squares of deviations between measured and fitted values for each ρV value used during calibration. Because the independent variable for this merit function is the value of A, we lower the input value A until the merit function reaches its minimum.

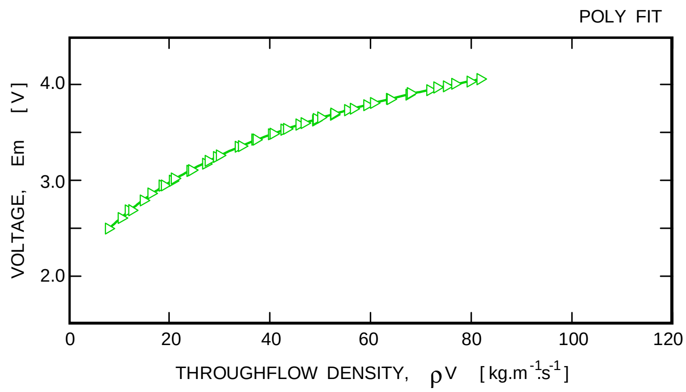

Fig. 6. Typical velocity calibration curve.

The simplicity of the King's law equation makes it easily usable for an inverse conversion of test data. Because King's law is based on flow and heat transfer physics, it can be expected that the conversion of voltages into flow velocities is reasonably accurate even slightly beyond the calibration range.

Lately a new method for fitting the velocity calibration of hot-wire data was introduced (Ref. 1). It is based on a polynomial fit of the 4th order as indicated by Eq. 2.

$$E = C_0 + C_1(\rho V) + C_2(\rho V)^2 + C_3(\rho V)^3 + C_4(\rho V)^4 \qquad \text{(Eq. 2)}$$

The polynomial fit is a pure mathematical construction with no physics involved. Therefore, its validity is strictly restricted only to the calibration region. Outside of this region, the polynomial can quickly reach unrealistic values. As will be shown shortly, the advantage of the polynomial calibration curve is that it is 'softer'; it follows the calibration data points sometimes better than does King's law.

To assess the goodness of King's law and the polynomial fit, we used calibration data as simulated test data and applied data conversion on these data. In an ideal case the results should be the ρV values of the calibration points. It should be mentioned here, that during the calibration process, about *5 s* of varying voltage data are taken. The voltage is averaged and this average is associated with a measured ρV value. This pair $(\rho V, E_M)$ represents coordinates of a single calibration point in the plot in Fig. 6. To evaluate King's law and polynomial fits, voltage conversions were carried out for both methods. After the conversion, the ρV records were averaged and compared with the corresponding input ρV values measured in the jet facility during the calibration process. The results in the form of deviations between averaged converted ρV values and the input values as a function of input (jet facility) ρV values are shown in Fig. 7 for the King's law and polynomial fit,

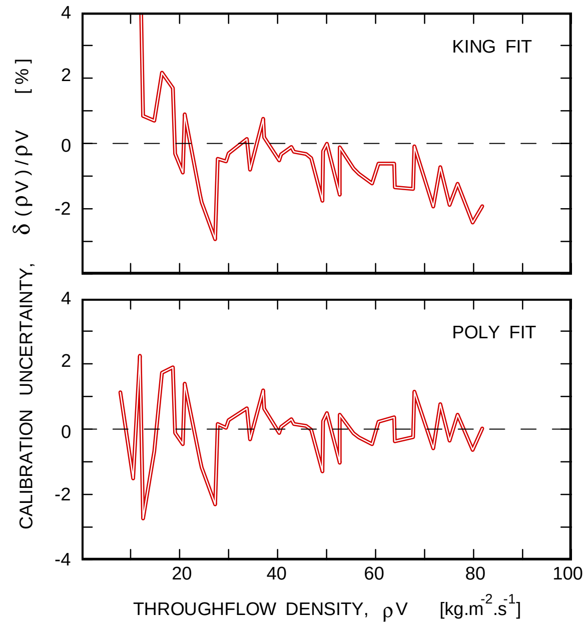

Fig. 7. Deviations between calibration and converted throughflow density values for King and polynomial calibration fits.

respectively. The results show that the polynomial fit exhibits lower deviations from the input data than does King's law. For this reason we used solely polynomial fits in our data conversion for all thermo-anemometric probes used in the course of this study.

The polynomial fit, however, has a big disadvantage during the data conversion; it requires solving an equation of the fifth order for each point to be converted (*125000* entries for each test point in our case). The equation is solved iteratively, and for large samples of data it can take a prohibitive amount of computer time. Thus an inverse form of polynomial fit is used

$$\rho V = D_0 + D_1E + D_2E^2 + D_3E^3 + D_4E^4 \qquad \text{(Eq. 3)}$$

This approach shifts computational difficulty to the evaluation of calibration data, however, a calibration curve usually does not consist of more than 40 points, so the required computer time is relatively short. Conversion of test voltages to the ρV values is now straightforward and very fast.

DIRECTIONAL CALIBRATION CHARACTERISTICS

The directional calibration procedure is applied to the split-fiber probes only. Single element probes, with a sensing cylinder perpendicular to the plane of two-dimensional flow are insensitive to a change of flow direction in this plane as long as the flow does not interfere with the probe prongs, which means an angular range of ±*90 dg* from the probe axial direction. As shown in detail in Ref. 8, the split-fiber probes exhibit a linear directional characteristic at least within the incidence angle range of ±*40 dg*. Even though the directional characteristic at a given flow Reynolds number is linear, its slope depends to certain extent on the flow Reynolds number, which for ambient conditions depends on the ρV value of the flow. A typical directional characteristic for both probe sensors is shown in Fig. 8. A differential directional characteristic for two values of ρV is shown in Fig. 9. It is the difference between the signal voltage of sensor #1 and the voltage of sensor #2 plotted as a function of the probe incidence angle. To capture this directional map mathematically, two functions were created. The first one is the characteristic slope as a function of flow ρV, and the second one is the residual voltage at zero incidence, also a function of flow ρV. Both functions are shown in Fig. 10, together with fitted curves using polynomials of the 4th order. As described in the following paragraph, these functions are used in the data reduction procedure for split-fiber probes.

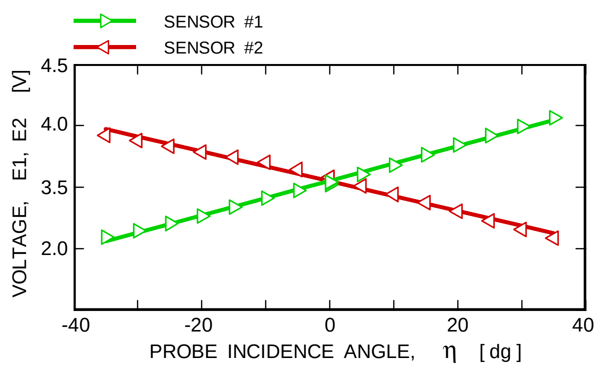

Fig. 8 Direction calibration a split-fiber probe at through-flow density of *58.8 kg.m^{-2}.s^{-1}* (*Re = 570*).

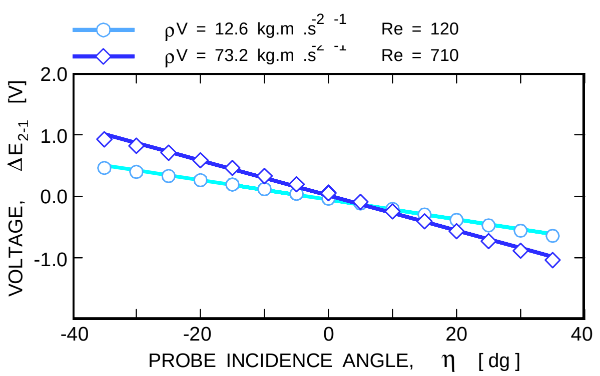

Fig. 9. Differential direction calibration characteristics of a split-fiber probe.

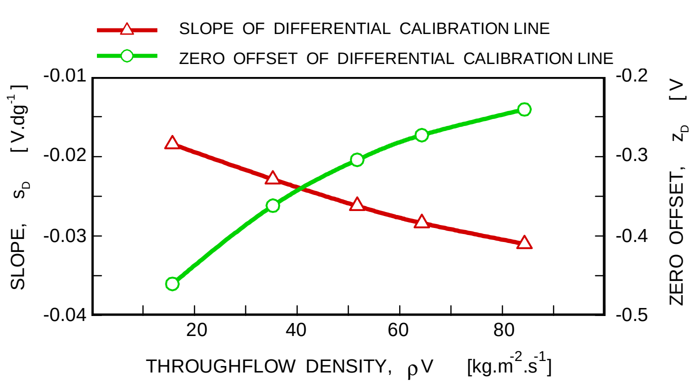

Fig. 10. Slope and zero offset of differential calibration lines as functions of throughflow density.

SIGNAL DECOMPOSITION PROCEDURE FOR SPLIT-FIBER PROBE

We have devised two procedures for the decomposition of split-fiber probe signals into velocity magnitude and velocity direction. The first procedure is described in detail in Ref. 8, and will only be outlined here. The procedure requires an initial guess of the flow throughflow density $(\rho V)_0$. Then, velocity direction is determined from the differential direction characteristic for the given ρV (slope, s_D, and residual voltage, z_D, functions are employed here). After that, voltages for zero flow incidence are determined from the directional characteristics of both sensors. In the next step, ρV values for each sensor are determined from velocity characteristics. Finally, the values $(\rho V)_1$ and $(\rho V)_2$ are compared, and if they are equal, or the difference is less than a prescribed threshold, the procedure stops. If the difference is larger a new input value $(\rho V)_0$ is calculated as an average of $(\rho V)_1$ and $(\rho V)_2$ and the entire process is repeated until the prescribed threshold on the throughflow density difference is satisfied. The procedure worked well in steady or mildly unsteady flow. However, for highly unsteady flows with large velocity and direction fluctuations, like flow in axial compressors for example, this procedure very often did not converge, and the difference threshold had to be raised to levels when resulting ρV values noticeable differed from averaged values determined by conventional aerodynamic probes. For this reason a new data reduction procedure was devised.

The new and currently used procedure is not an iterative process but it is based on the minimum value of a merit function that is built over the entire range of ρV values for which the probe was calibrated as follows. First, the voltage difference from test data between sensors #1 and #2 is determined. Then, the procedure scans through the range of ρV values, and determines the incidence angles from differential directional characteristic for the voltage difference $\Delta E_{2\text{-}1}$ and a particular ρV value (Fig. 9). Now, the voltage difference $E2 - E1$ can be determined from individual directional characteristics for the incidence angle and a ρV value (Fig. 8). The value of the merit function is calculated as the square of difference between $\Delta E_{2\text{-}1}$ and $E2 - E1$. The particular $(\rho V)_M$ value, for which the merit function reaches its minimum, is the throughflow density value of the flow. As seen here, the entire process is performed in the domain of directional characteristics. Now, knowing the incidence, the test data voltages can be corrected for directional effects, and resulting voltages are used as inputs into velocity characteristics of both sensors on the probe to determine $(\rho V)_1$ and $(\rho V)_2$ values (Fig. 6). Finally, the flow throughflow density value is calculated as an average of $(\rho V)_1$, $(\rho V)_2$ and $(\rho V)_M$. Ideally, these three values are identical; in reality they differ usually within *3%* of their average value. These three values are monitored during the data reduction process. Test data for which the difference among these values is larger than *3%* are discarded. The procedure is very fast; to reduce a data set of 160000 entries takes about *90 s* on a current PC. Of course, there are no convergency problems with this procedure.

MEASUREMENT IN FREE-JET FACILITY

The first evaluation of the split-fiber probe performance and signal decomposition was carried out in the free-jet facility. Flow in a free jet is predominantly one dimensional in the jet initial region (potential core). Probes traversed the free-jet stream at a station *34 mm* downstream of the nozzle exit plane ($x/D_J = 0.89$). Velocity profiles measured by three probes (single-wire, single-fiber, and split-fiber probe) are shown in Fig. 11a. The probe velocity data are normalized by the characteristic jet-exit velocity V_J, which was determined from total pressure measured in the plenum ahead of the nozzle and the ambient pressure of the surrounding air. All three probes performed extremely well as far as the velocity magnitude is concerned. There is a very small difference in determining the jet stream width (within *2%* of the nozzle exit radius. The differences in the jet velocity value within the jet potential core are within *1%* of V_J for all three cases.

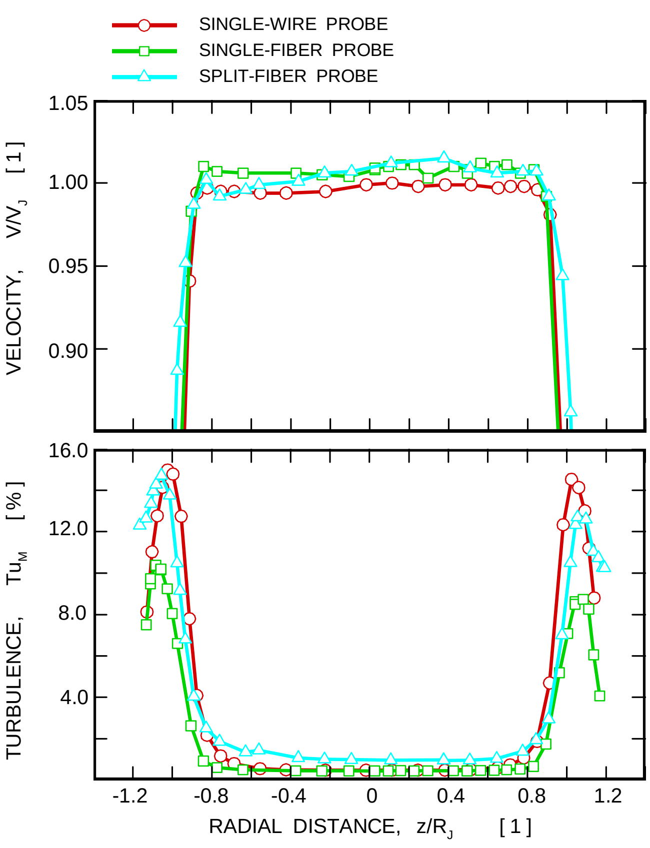

Fig. 11a,b. Mean velocity and turbulence in the jet stream measured by three anemometric probes.

The accompanying distributions of velocity unsteadiness are presented in Fig. 11b. Velocity unsteadiness, in this case velocity turbulence, was determined as a ratio of the RMS of velocity fluctuations to the jet-exit characteristic velocity V_J. As seen in Fig. 11b, all three probes determined the location of the peak of velocity unsteadiness quite closely (within *3%* of the nozzle exit radius). However, there are visible differences in the peak values of measured velocity unsteadiness in the jet shear layer. Specifically, the peak values are *14.7%* for the single-wire probe, *9.5%* for the single-fiber probe, and *13.7%* for the split-fiber probe (the values indicated are averages for the left and right jet shear layer). While the split-fiber probe and the single-wire probe indicate turbulence levels that are very close, the single-fiber probe determined a turbulence level that is visibly lower. This difference indicates that the single-fiber probe exhibits noticeably lower sensitivity to velocity fluctuations than other probes. The frequency response of the single-wire probe was determined using a square-wave test (Ref. 1). The test indicated that the wire probe has a flat characteristic (within *3 dB*), up to a cut-off frequency of *75 kHz*. For hot-film probes, however, the theory of the square wave test has not yet been developed (Ref. 12). The complication is the thermal inertia of the substrate (fiber). It is generally accepted that the hot-film probes have noticeably lower cut-off frequency than hot-wire probes. Also, it has been established that the cut-off frequency of single wire probes drops with increasing wire diameter. In the case of fiber hot-film probes, however, the situation is different. Surprisingly, within a certain diameter range, the cut-off frequency increases with increasing fiber diameter (Ref. 12). It is due to the fact that with fiber probes, only a very thin film on the fiber surface is heated, while the core (the fiber) is not because of its very low heat conductivity. This may explain a higher sensitivity to velocity fluctuations for a split-fiber probe in comparison with a single-fiber probe turbulence data (Fig. 11b). It seems, that for turbulence levels of up to *15%* for velocity up to Mach number of *0.2*, the frequency response of the split-fiber probe is comparable with the single-wire probe. In any case, the frequency response of fiber probes requires further study.

The split-fiber probe was also investigated for sensitivity to probe setting angle. Figs. 12 and 13 show the results of this test. The effect of probe setting angle on the measured flow angle is plotted in Fig. 12. The true flow angle for this flow is *0 dg*. As seen here, the probe and the signal decomposition procedure work well for a relatively wide range of setting angles about the probe zero incidence. The measured flow angle deviates from the true flow angle less than *1 dg* for a

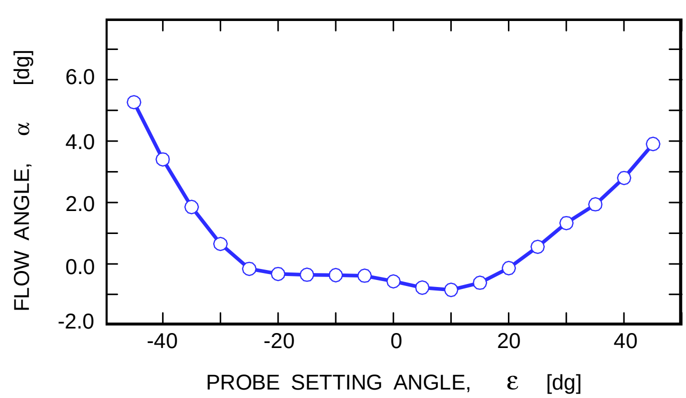

Fig. 12. Measured flow angle as a function of setting angle of a split-fiber probe.

range of probe setting angles from *-30 dg* to *+25 dg*. The effects of setting angle on measured flow velocity exhibit a lopsided distribution as seen in Fig. 13. The measured velocity values are within *1%* of the jet velocity for a range of setting angles between *-20 dg* to *+10 dg* and within *2%* accuracy for a range of setting angles from *-40 dg* to *+14 dg*. Reasons for the asymmetry in the velocity readings are not known. Measurement of turbulence intensity (velocity fluctuations) is affected very little by the probe setting in the entire range from *-45 dg* to *+45 dg*. In summary, the split-fiber probe and the signal decomposition procedure work well for the case of a jet flow. The probe can determine the flow velocity with *1%* accuracy for the velocity range from *10* to *80* $m.s^{-1}$, and flow angles with an accuracy of *1 dg* for a range of flow angles from *-20 dg* to *+10 dg* with respect to the probe zero incidence. Extra precaution must be taken if the probe is used beyond this range of flow conditions.

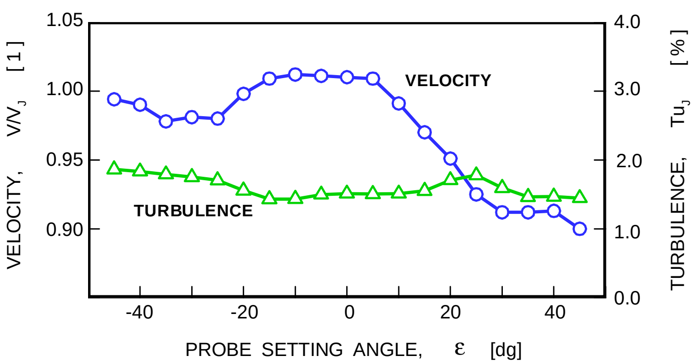

Fig. 13. Measured velocity and turbulence as functions of setting angles of a split-fiber probe.

MEASUREMENT IN THE LSAC FACILITY

In the second phase of verification tests, the thermo-anemometric probes were used in the NASA LSAC facility. Probes were traversed in the radial (spanwise) direction at a given circumferential position in the gap between the first rotor and stator (Fig. 1). The resulting radial profiles of mean velocity were used for the verification of probe and signal decomposition performance. There are, however, certain factors that complicate this verification process. First, flow in this facility, as in any axial compressor, is inherently unstable, and flow parameters are not known in advance with the same degree of accuracy as in the case of a free jet. The thermo-anemometric data were averaged in time, and compared to data acquired by conventional pneumatic probes. However, pneumatic probes in unsteady flows do not necessarily supply a true average value of the measured parameters. In the case of pressure probes, for example, the deviations from the true average value depend on the probe and connecting tubing layout, and usually they are not exactly known. Further, the flow average velocity value is determined from parameters that were averaged in the pressure and temperature domains. On the other hand, the average velocity value based on thermo-anemometric data is the true velocity average because the averaging process is done mathematically in the unsteady velocity domain.

Another complication in these verification tests is the fact that the flow in the compressor annulus is not uniform in the tangential (pitchwise) direction but depends on the relative position of the probe and stator blades in the downstream cascade. We have only two ports available for thermo-anemometric probes in the LSAC facility. In the first port, the probes traverse the flow at a midpitch position (Fig. 1, pos. A); in the second port, the probes are at a position upstream of a stator blade (Fig. 1, pos. B). All thermo-anemometric data presented here were acquired at position A. The pneumatic probes, however, can traverse the compressor channel at many different circumferential positions over several blade pitches, and the resulting radial profile is an average of all these traverses. The effects of circumferential nonuniformity on the representative average radial profiles of mean velocities are suppressed this way.

Data acquired by a split-fiber probe at position A are shown in Fig. 14. Plots of velocity magnitude, and axial and tangential components are shown in the left half of the figure. The velocity unsteadiness plots are in the right half of Fig. 14. It must be stressed here that these plots do not show flow turbulence, because they were acquired in the absolute flow system, and consequently the velocity unsteadiness also contains the contribution of the deterministic velocity fluctuations due to the passage of wakes. The plot at the top shows both the unsteadiness of velocity magnitude fluctuations, as well as the overall velocity unsteadiness that contains contributions of magnitude and angle fluctuations (labeled *AXI+TAN*). The difference between velocity magnitude and overall unsteadiness was explained earlier (Fig. 4). The velocity magnitude unsteadiness is shown for comparisons with single-element thermo-anemometric probes.

The results of measurements at port A for three thermo-anemometric probes are shown in Fig. 15. Again, the plots are velocity magnitude on the left, and unsteadiness on the right. The upper pair of plots is for a single-wire probe, the middle one for the single-fiber probe, and the lower pair of plots is for the split-fiber probe. The shape of the velocity magnitude profile is practically identical for all three probes, the differences are less than *2%* of a velocity value. It should be emphasized here that the data reduction procedure for the single-fiber and single wire probes is a straightforward polynomial conversion that does not involve the decomposition procedure introduced here for the split-fiber probe. These results confirm the validity of the signal decomposition procedure for the split-fiber probe.

The other aspect of this excellent agreement and also the agreement for the free-jet case (Fig. 11), that all three probes measure unsteady velocity reliably even under conditions of

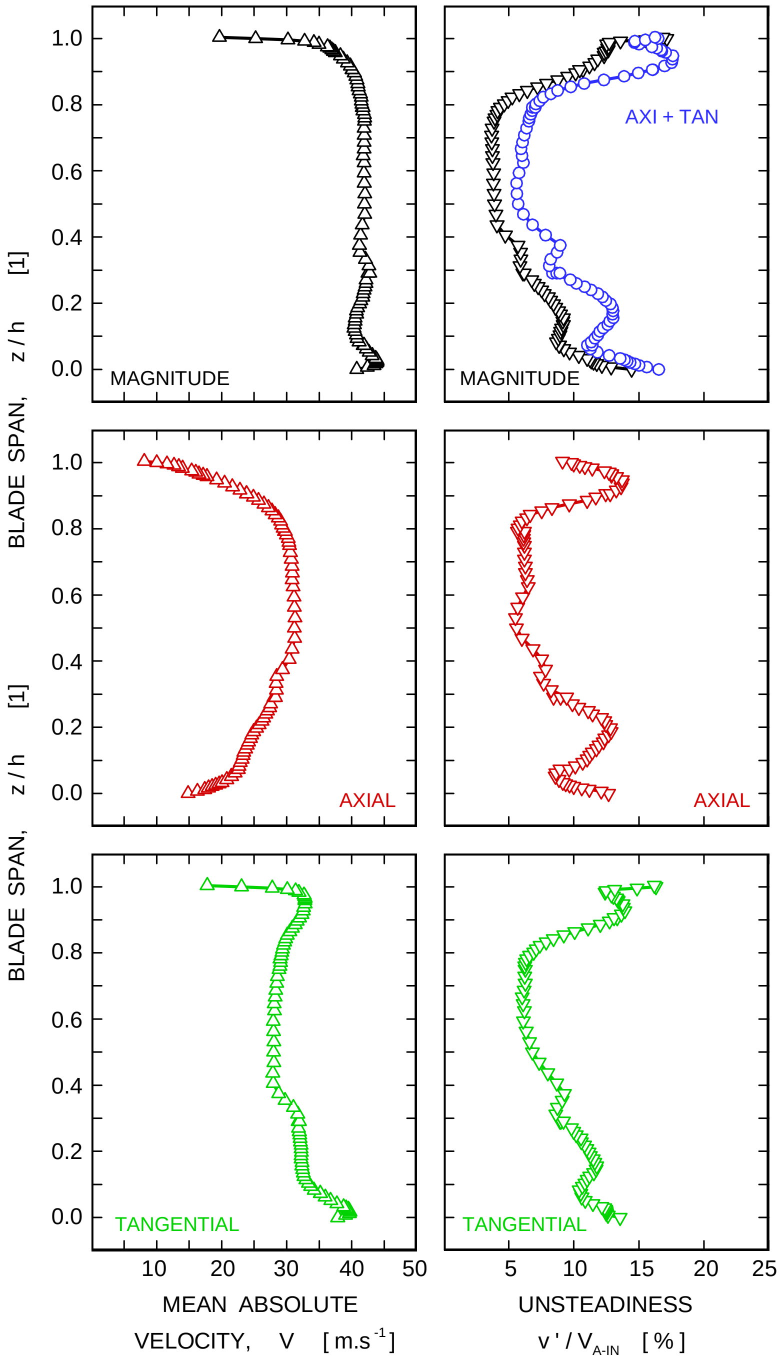

Fig. 14. Spanwise distribution of absolute flow velocity and velocity unsteadiness in the gap between the first rotor and stator blade row measured by split-fiber probe.

extremely high unsteady flow. This finding indicates that there is practically no difference in operation of a thin wire on one side and a relatively thick fiber on the other side under unsteady flow conditions in comparison with operation in steady flows. Operation of these probes is based on heat transfer from the sensing element. Obviously, there is not a significant change in the sensor heat transfer between the steady flow of a free jet and highly unsteady flow in the compressor stage. The heat transfer rate from a cylinder in cross flow is affected by the flow pattern around the cylinder. There are dramatic changes in the flow pattern as the Reynolds number increases, particularly in the very low Reynolds number region. In the range from *Re = 2* to *Re = 23*, which is the range where the single-wire probe operates, there is a symmetric recirculation zone with two attached vortices behind the cylinder. For a Reynolds number about *50*, the Kármán vortex street sets in behind the cylinder, and for flows above *Re = 400*, there is a fully turbulent wake behind the cylinder Ref. 11). The single-fiber and split-fiber probes operate in the Reynolds number range from *25* to *300* and from *75* to *1000*, respectively. Therefore, these probes operate in the range of transition between flow patterns around the sensing element. The values of transition Reynolds numbers were established for uniform and steady inflows. It seems that high velocity unsteadiness has little effect on the values of the transition Reynolds numbers in the low Reynolds number range. At present, this is a purely speculative suggestion that must be verified experimentally.

The average velocity profile acquired by the conventional pneumatic probe is shown in Fig. 16. The agreement between the pneumatic probe data and data for the thermo-anemometric probes shown in left-hand plots in Fig. 15, is excellent; the differences are less than *1%*. This agreement, however, is probably only fortuitous, because as explained earlier the profile in Fig. 16 is an average of 41 profiles measured at different pitch positions. The spread of data from the conventional probes is also indicated in Fig. 16 by the curves on both side of the velocity profile. The spread of the pneumatic probe data is *±5%*, which is much larger than the spread of the data among the three thermo-anemometric probes. The data spread for the pneumatic probe was caused by varying the probe position along the stator row blade pitch, while for the thermo-anemometric probes it is due to the differences among the probes.

All three thermo-anemometric probes indicated also a very similar distribution of velocity magnitude unsteadiness (Fig. 15). The differences among unsteadiness data for all these probes are similar to those observed in the free jet measurements. Again, the single-fiber probe indicates overall slightly lower velocity unsteadiness levels than the other two probes, which is consistent with the results from the shear layer of a free jet. Regardless of the differences in response characteristics of thermo-anemometric probes, the results presented demonstrate that all these probes are suitable for unsteady velocity measurements in the NASA LASC facility.

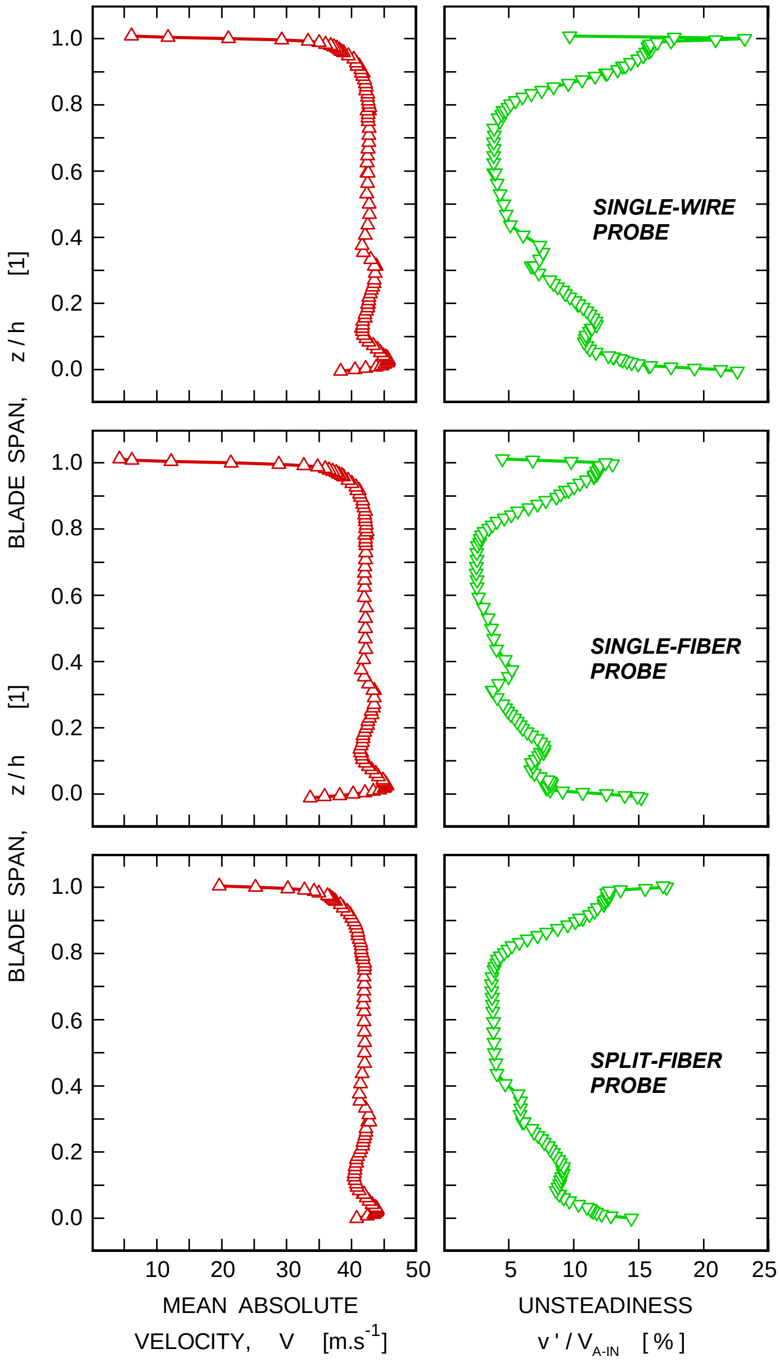

Fig. 15. Spanwise distributions of absolute flow velocity and velocity unsteadiness measured by three thermo-anemometric probes.

Finally, the results of flow angle measurements are presented in Fig. 17, for the split-fiber probe and a conventional nulling wedge probe. Both probes indicate similar distributions of absolute flow angles along the blade span. The double line in the plot shows the distribution of the stator blade leading edge angles along the blade span as seen by the incoming flow. It should be mentioned again, that the split-fiber probe data are for a single radial traverse, while the

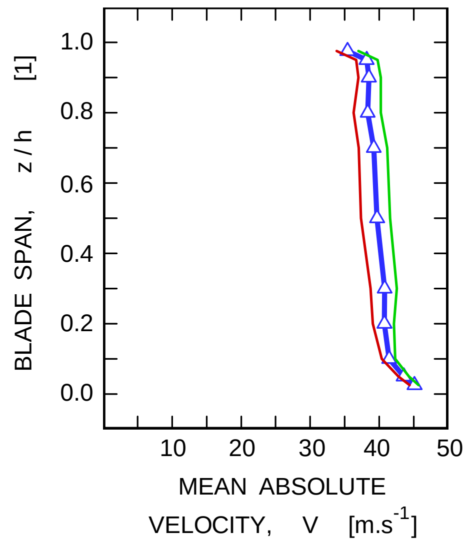

Fig. 16. Spanwise distribution of absolute flow mean velocity behind the first rotor measured by pneumatic probes.

wedge-probe data represents an average of 41 radial traverses. The maximum and minimum values of this set of wedge probe traverses are indicated in the plot. It is generally accepted that the accuracy of angle measurement with a nulling wedge probe suffers in flows with a very high intensity of unsteadiness. In the case of the LSAC facility, this occurs mainly in the upper half of the blade span $z/h > 0.8$ (see Fig. 15), where the wedge probe indicates slightly larger flow angle than the split-fiber probe. In the lower half of the blade span $z/h < 0.5$, the agreement between data from these two probes is quite good.

CONCLUSIONS

The following were achieved during the course of this study in which three different thermo-anemometric probes were used for velocity measurement in free-jet and LSAC facilities.

- A calibration method was devised for a split-fiber probe that consists of a single velocity calibration at zero probe incidence and several directional calibrations at different velocities.
- A new algorithm was developed to decompose split-fiber probe signals into velocity and flow direction. The algorithm is based on the minimum value of a merit function that is built over the entire range of flow velocities for which the probe was calibrated. The new decomposition scheme is fast and robust.

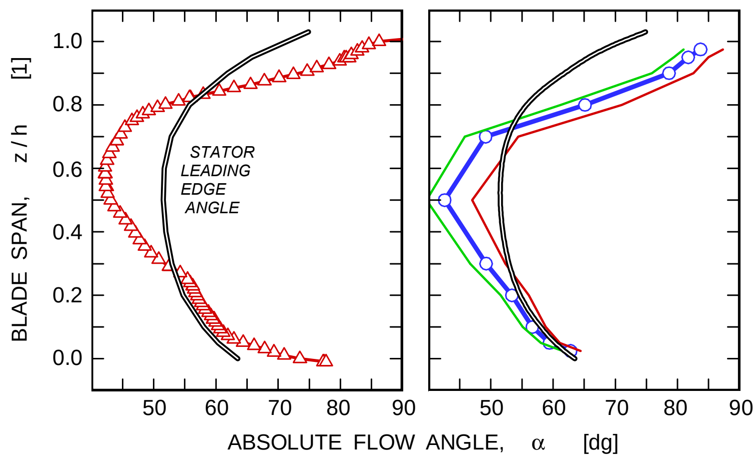

Fig. 17. Spanwise distribution of absolute flow velocity angle in the gap between the first rotor and stator blade row measured by split-fiber and wedge probes.

- The split-fiber probe performance and signal decomposition was first verified in the free-jet facility by comparing the data among three thermo-anemometric probes. All three probes performed extremely well as far as the velocity magnitude was concerned; the differences among these data are within *1%*. However, there are visible differences in the peak values of measured velocity unsteadiness in the jet shear layer, in particular the single-element fiber probe determined a turbulence level that is visibly lower, which indicates that this probe has low sensitivity to velocity fluctuations.

- The experiments in the LSAC facility showed that all three thermo-anemometric probes detect the same velocity magnitude; the differences among these probes are less than *2%* of the velocity value. The differences among measured unsteadiness levels are similar to those observed in the free jet measurements. Mean velocity and flow angle distributions measured by thermo-anemometric probes agree very well with data measured by conventional pneumatic probes. These findings boost our confidence in the correctness of unsteady velocity data measured by thermo-anemometric probes in the LSAC environment.

- In summary, the split-fiber probe worked reliably during the entire program. The acquired data averaged in time followed closely the data acquired by conventional pneumatic probes. Despite small differences among all probes used, that still need to be explained, it is believed that data acquired by split-fiber probe can be used reliably to analyze unsteady flow phenomena in the NASA Low Speed Axial Compressor.

REFERENCES

1. Bruun, H.H.: "Hot-Wire Anemometry, Principles and Signal Analysis', Oxford University Press Inc., New York, 1995.
2. Richter, H.: "Measurement of Two-Dimensional Periodic Flow Behind Turbine Guide-Vanes by Means of a Split-Fiber Probe", Dantec Information, no.1, pp.10-12, 1985.
3. Helle, L.: "The use of a split-fiber probe for aerodynamic research", Dantec Information, no.12, pp.17-20, 1993.
4. Falk A.E., Jumper, E.J, Fabian, M.K., and Stermer, J.: "Upstream-Propagating Potential Disturbances in the F109 Turbofan Engine Inlet Flows", *Journal for Propulsion and Power*, Vol. 17, No. 2, pp. 262-269, 2001.
5. Tong, J., Zhe, Y., and Liang, L.Z.: "Flow Fields behind Centrifugal Impellers", Dantec Information No. 7, pp. 8-9, 1989.
6. Bendali, M.: "The use of a Dantec 55P11 slanted hot-wire probe for the measurement of three-component velocities behind a twisted eight-bladed axial fan", Dantec Information No. 14, pp. 20-21, 1995.
7. Wasserbauer C.A., Weaver, H.F., and Senyitko, R.G.: "NASA Low-Speed Axial Compressor for Fundamental Research", NASA TM-4635, 1995.
8. Lepicovsky, J.: "Application of a Split-Fiber Probe to Velocity Measurement in the NASA Research Compressor", ASME paper FEDSM2003-45607, 2003.
9. Dantec Probe Catalog, Publ. No. 2201E, Dantec Electronics Inc., 1982.
10. Norman, B.: "Hot-wire Anemometer Calibration at high Subsonic Speeds", DISA Information, No.5, pp.5-19, 1967.
11. Van Dyke, M.: "An Album of Fluid Motion", Parabolic Press, Stanford, California, 1982.
12. Freymuth, P. and Fingerson, L.M.: "Electronic testing of frequency response for thermal anemometers", TSI Quarterly, Nov. 1977.

REPORT DOCUMENTATION PAGE

Form Approved
OMB No. 0704-0188

1. AGENCY USE ONLY (*Leave blank*)

2. REPORT DATE
April 2004

3. REPORT TYPE AND DATES COVERED
Final Contractor Report

4. TITLE AND SUBTITLE
Measurements With a Split-Fiber Probe in Complex Unsteady Flows

5. FUNDING NUMBERS
WBS–22–708–28–03
NAS3–00145

6. AUTHOR(S)
Jan Lepicovsky

7. PERFORMING ORGANIZATION NAME(S) AND ADDRESS(ES)
QSS Group, Inc.
21000 Brookpark Road
Cleveland, Ohio 44135

8. PERFORMING ORGANIZATION REPORT NUMBER
E–14531

9. SPONSORING/MONITORING AGENCY NAME(S) AND ADDRESS(ES)
National Aeronautics and Space Administration
Washington, DC 20546–0001

10. SPONSORING/MONITORING AGENCY REPORT NUMBER
NASA CR—2004-213065
GT–2004–53954

11. SUPPLEMENTARY NOTES
Prepared for the Turbo Expo 2004 sponsored by the American Society of Mechanical Engineers, Vienna, Austria, June 14–17, 2004. Project Manager, Eric R. McFarland, Turbomachinery and Propulsion Systems Division, NASA Glenn Research Center, organization code 5810, 216–433–5915.

12a. DISTRIBUTION/AVAILABILITY STATEMENT
Unclassified - Unlimited
Subject Categories: 02 and 07 Distribution: Nonstandard
Available electronically at http://gltrs.grc.nasa.gov
This publication is available from the NASA Center for AeroSpace Information, 301–621–0390.

12b. DISTRIBUTION CODE

13. ABSTRACT ***(Maximum 200 words)***
A split-fiber probe was used to acquire unsteady data in a research compressor. A calibration method was devised for a split-fiber probe, and a new algorithm was developed to decompose split-fiber probe signals into velocity magnitude and direction. The algorithm is based on the minimum value of a merit function that is built over the entire range of flow velocities for which the probe was calibrated. The split-fiber probe performance and signal decomposition was first verified in a free-jet facility by comparing the data from three thermo-anemometric probes, namely a single-wire, a single-fiber, and the split-fiber probe. All three probes performed extremely well as far as the velocity magnitude was concerned. However, there are differences in the peak values of measured velocity unsteadiness in the jet shear layer. The single-wire probe indicates the highest unsteadiness level, followed closely by the split-fiber probe. The single-fiber probe indicates a noticeably lower level of velocity unsteadiness. Experiments in the NASA Low Speed Axial Compressor facility revealed similar results. The mean velocities agreed well, and differences in the velocity unsteadiness are similar to the case of a free jet. A reason for these discrepancies is in the different frequency response characteristics of probes used. It follows that the single-fiber probe has the slowest frequency response. In summary, the split-fiber probe worked reliably during the entire program. The acquired data averaged in time followed closely data acquired by conventional pneumatic probes.

14. SUBJECT TERMS
Thermoanemometry; Unsteady flow velocity; Axial compressor

15. NUMBER OF PAGES
17

16. PRICE CODE

17. SECURITY CLASSIFICATION OF REPORT	18. SECURITY CLASSIFICATION OF THIS PAGE	19. SECURITY CLASSIFICATION OF ABSTRACT	20. LIMITATION OF ABSTRACT
Unclassified	Unclassified	Unclassified	